Experimental and theoretical analysis of integrated circuit (IC) chips on flexible substrates subjected to bending

Ying Chen, Jianghong Yuan, Yingchao Zhang, Yonggang Huang, and Xue Feng

Citation: Journal of Applied Physics **122**, 135310 (2017); doi: 10.1063/1.4986882
View online: https://doi.org/10.1063/1.4986882
View Table of Contents: http://aip.scitation.org/toc/jap/122/13
Published by the American Institute of Physics

Experimental and theoretical analysis of integrated circuit (IC) chips on flexible substrates subjected to bending

Ying Chen,[1,2] Jianghong Yuan,[3] Yingchao Zhang,[1] Yonggang Huang,[4,a)] and Xue Feng[1,a)]
[1]*Department of Engineering Mechanics, Center for Mechanics and Materials, Tsinghua University, Beijing 100084, China*
[2]*Center for Nano and Micro Mechanics, Tsinghua University, Beijing 100084, China*
[3]*School of Mechanics and Engineering, Southwest Jiaotong University, Chengdu 610031, China*
[4]*Department of Civil and Environmental Engineering and Department of Mechanical Engineering, Northwestern University, Evanston, Illinois 60208, USA*

(Received 7 June 2017; accepted 19 September 2017; published online 6 October 2017)

The interfacial failure of integrated circuit (IC) chips integrated on flexible substrates under bending deformation has been studied theoretically and experimentally. A compressive buckling test is used to impose the bending deformation onto the interface between the IC chip and the flexible substrate quantitatively, after which the failed interface is investigated using scanning electron microscopy. A theoretical model is established based on the beam theory and a bi-layer interface model, from which an analytical expression of the critical curvature in relation to the interfacial failure is obtained. The relationships between the critical curvature, the material, and the geometric parameters of the device are discussed in detail, providing guidance for future optimization flexible circuits based on IC chips.

https://doi.org/10.1063/1.4986882

INTRODUCTION

Stretchable and flexible electronics have been the focus of current research due to their novel features compared with more typical planar electronic devices, especially their ability to directly integrate with the human body in a conformal way.[1–6] Thus, all kinds of stretchable and flexible sensors,[7–20] actuators,[13,21] and energy supply devices[3,22–26] which are thin, soft, and easily integrated with the human body have been developed for wearable physiological monitoring and disease therapy. However, due to the diversity and high density of the circuits required in integrated circuit (IC) chips which are capable of data acquisition, processing, and transmission, their transformation into stretchable and flexible devices is still challenging. Therefore, for stretchable devices that are intended to work on the human body by intimate contact in a continuous and wireless style, integrating IC chips on a flexible substrate has become the solution, which facilitates the applications of stretchable and flexible devices in clinical medicine and basic science of medicine research.[27–29]

A known flexible substrate which is ready to accommodate IC chips is the flexible printed circuit board (FPCB). This has already been used as a replacement for the conventional printed circuit board (PCB) as a space and weight saving solution. It can also act as the connections of dynamic elements in electronics, for example, in camera lenses. Various mechanical analyses and experiments have been carried out to study performance and reliability in the case of static or dynamic deformation. When an FPCB acts as the dynamic connections, its failure in the conducting layer due to periodic bending has been studied both experimentally and numerically.[30,31] When the FPCB with a reduced thickness and stiffness serves as an alternative for the rigid PCB, drop tests and the fluid-structure interaction analysis have been conducted to investigate its response.[32–34] Moreover, there are millimeter-sized robots based on the FPCB integrated with actuators, sensors, and power supply chips, where the FPCB is folded to reduce the total size of the robot.[35] These studies on IC chips integrated with flexible substrates focus either on the functionality of the flexible substrate or on the dynamic response in the drop test or the fluid-structure interaction. However, few are concerned with the case in which the IC chips are designed to work on curved surfaces such as the human body. In such a case, the failure of IC chips on a bent flexible substrate due to the material/geometric mismatch will determine the whole device's performance and reliability. Therefore, the study on IC chip integrated flexible devices subjected to curvature is necessary for their applications. The interfacial failure analysis based on multilayer structure mechanics has been of much importance to both traditional and flexible electronic devices.[36–39]

Should the flexible substrate be bent, the junction area at the edge of the IC chip would be the weakest part in the device due to the sudden geometric change in the profile and the existence of the interface, which in turn will limit the bendability of the whole device. In this paper, a strategy is proposed to analyze the interfacial failure of IC chips integrated with a flexible substrate under bending deformation, theoretically and experimentally. We first develop a compressive buckling-based experimental method to quantitatively load the device with a certain curvature at the junction edge. The curvature can be easily modulated by the size of the device and the compressive ratio. This experimental method can be used to evaluate the reliability of the IC chip-based

a)Authors to whom correspondence should be addressed: y-huang@northwestern.edu and fengxue@tsinghua.edu.cn

flexible devices. A theoretical model based on the beam theory and the bi-layer interface model is also established to study the interfacial failure, especially the relationship between the energy release rate at the interface and the bending deformation. The dependence of the device's bendability (defined as the maximum curvature) on the geometry, material, and interfacial toughness is analyzed and discussed in detail. This theoretical model can be used to predict the bendability of the IC chip based flexible devices. Hopefully, the experimental and theoretical analysis developed in this paper can provide valuable guidance for the optimization of IC chip based flexible devices, and thus facilitate the potential application of stretchable and flexible electronics.

COMPRESSIVE BUCKLING EXPERIMENT

Hybrid integration of the stretchable and flexible electronic sensors and actuators with the IC chip based flexible circuits, as shown in Fig. 1(a), can improve both the comfort and accuracy of the devices in healthcare applications. The failure of IC chips on the flexible substrate may occur in the fracture of the circuits defined by the conducting material buried in the flexible substrate, the fracture of the bonding material, or the debonding of the IC chip's substrate interface; the latter of these is the most common and will be the focus here. IC chips are encapsulated generally with the aid of a bonding layer (e.g., soldering or conductive adhesive)

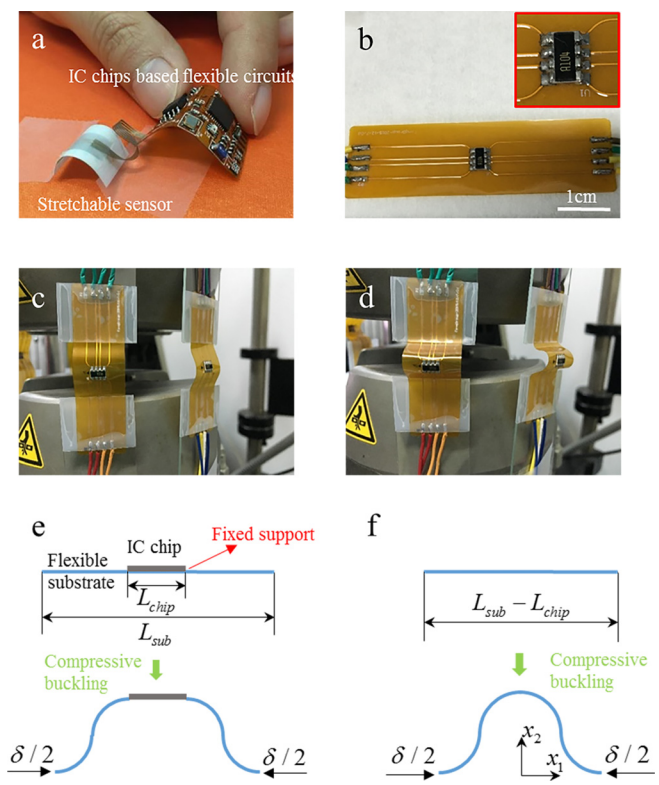

FIG. 1. The compressive buckling test of the device. (a) Photograph of the wearable device composed of the stretchable sensor and the IC chip-based flexible circuits. (b) Photograph of the device to be tested, and the inset shows the detail of the IC chip integrated onto the flexible substrate by soldering. (c) The initial state of the device in each compressive buckling cycle. (d) The final state of the device in each compressive buckling cycle. (e) The theoretical illustration of the device in compressive buckling. (f) The equivalent model after simplification.

but usually in different styles due to their varied structures. As a result of the sudden geometric change, the bonding at the corners of the IC chip is prone to the stress concentration in the case of deformation. Moreover, the existence of the interface makes it the weakest in the integrated device, which degrades the bendability of the whole device. Here, the compressive buckling experiment, also used in the thin film characterization and the three-dimensional (3D) structure manufacturing, is proposed to impose a quantitative bending deformation at the bonding edge of IC chips on the flexible substrate. The deformation and strain state at the local bonding edge in compressive buckling can be assumed to be like that of the condition of pure bending.

For simplification, a multi-resistor chip is used to represent the IC chips and the polyimide thin film with a predefined circuit acting as the flexible substrate, as shown in Fig. 1(b). The inset of Fig. 1(b) shows the multi-resistor chip, which is composed of four independent resistors, and the failure of each can be measured by their resistance change. A fatigue testing machine is used to conduct compressive displacement, denoted as δ, at the ends of the device to induce its buckling, as shown in Figs. 1(c) and 1(d). For convenience, the compressive ratio, denoted as λ, is introduced as the ratio of the compressive displacement to the effective length of the device. Figure 1(c) shows the initial state of the device where $\delta_0 = 1\,\text{mm}$ and $\lambda_0 = 5\%$, and Figure 1(d) shows the final state of the device in each loading cycle where $\delta_{\max} = 8\,\text{mm}$ and $\lambda_{\max} = 40\%$. It can be observed that, as the compressive displacement increases, the wavelength of the buckled device decreases while its amplitude increases, and the curvature at the bonding edge of the IC chip also increases.

The curvature at the bonding edge of the IC chip can be predicted by the two-dimensional (2D) buckling theory quantitatively, once the compressive displacement and the size of the device are known. The theoretical model is illustrated in Fig. 1(e), in which the length of the IC chip and the flexible substrate are denoted as L_{chip} and L_{sub}, respectively. Since the bending stiffness of the IC chip is much larger than that of the flexible substrate due to the thickness difference, it is reasonable to assume that the flexible substrate is totally fixed at the bonding edge, where both the deflection and rotation angles are zero. Therefore, the problem described in Fig. 1(e) is equivalent to that in Fig. 1(f) where the IC chip is removed and the device is simplified as a shortened flexible substrate with an effective length of $L_{\text{sub}} - L_{\text{chip}}$. Once the compressive displacement exceeds some critical value, the device would buckle toward the IC chip's direction with delicate control.

The deformation of the device can be solved as a small strain problem with large rotations under the plane-strain assumption. In the rectangular coordinates (x_1, x_2) attached to Fig. 1(f), the deflection of the buckled device can be approximated by

$$u_2 = \frac{A}{2}\left(1 + \cos\frac{2\pi x_1}{L}\right), \quad -\frac{L}{2} \le x_1 \le \frac{L}{2}, \tag{1}$$

where A is the buckling amplitude to be determined, and $L = L_{\text{sub}} - L_{\text{chip}}$ is the effective length as shown in Fig. 1(f).

The normal strain in the direction of x_1 in the flexible substrate can be expressed as

$$\varepsilon_{11} = \varepsilon_{11}^0 + x_2\kappa_{11}, \tag{2}$$

where $\kappa_{11}(x_1) = -\partial^2 u_2/\partial x_1^2$ is the curvature of the buckled flexible substrate and $\varepsilon_{11}^0 = \partial u_1/\partial x_1 + \sin(2\pi x_1/L)\pi^2 A^2/2L^2$ is the axial strain, with u_1 being the axial displacement of the flexible substrate. The membrane force per unit width in the flexible substrate can be expressed in terms of the axial strain as

$$N_{11} = \bar{E}h\varepsilon_{11}^0, \tag{3}$$

in which h is the thickness of the flexible substrate, and $\bar{E} = E/(1-\nu^2)$ is the plane-strain modulus dependent on Young's modulus E (referred to as modulus hereinafter) and Poisson's ratio, ν. Since the shear stress on the bottom and top surfaces of the flexible substrate is zero, we have $\partial N_{11}/\partial x_1 = 0$ according to the force equilibrium. The boundary condition can be written as $u_1(0) = 0$, $u_1(L/2) = -\delta/2$ due to the symmetry of the problem. Therefore, the axial displacement u_1 can be calculated as

$$u_1 = -\frac{\delta}{L}x_1 + \frac{\pi A^2}{16L}\sin\left(\frac{4\pi x_1}{L}\right). \tag{4}$$

Using Eqs. (1) and (4), the membrane strain energy U_m and the bending strain energy U_b per unit width can be derived, respectively, as

$$U_m = \int_{-\frac{L}{2}}^{\frac{L}{2}} \frac{1}{2}N_{11}\varepsilon_{11}dx_1 = \frac{\bar{E}hL}{2}\left(\frac{\pi^2A^2}{4L^2} - \frac{\delta}{L}\right)^2, \tag{5}$$

$$U_b = \int_{-\frac{L}{2}}^{\frac{L}{2}} \frac{\bar{E}I_1}{2}\kappa_{11}^2 dx_1 = \frac{\bar{E}I_1A^2\pi^4}{L^3}, \tag{6}$$

where $I_1 = h^3/12$ is the moment of inertia per unit width of the flexible substrate. The total elastic energy per unit width can thus be expressed as $\Pi = U_m + U_b$. Finally, minimizing the energy Π gives the buckling amplitude as

$$A = 2\sqrt{\frac{\delta L}{\pi^2} - \frac{h^2}{3}}. \tag{7}$$

Therefore, the deflection and the curvature of the buckled flexible substrate can be represented as

$$u_2 = \sqrt{\frac{\delta L}{\pi^2} - \frac{h^2}{3}}\left(1 + \cos\frac{2\pi x_1}{L}\right) \tag{8}$$

and

$$\kappa_{11} = \frac{4\pi^2}{L^2}\sqrt{\frac{\delta L}{\pi^2} - \frac{h^2}{3}}\cos\left(\frac{2\pi x_1}{L}\right), \tag{9}$$

respectively.

Obviously, the bending curvature given in Eq. (9) reaches its maximum,

$$\kappa_{11\max} = \frac{4\pi^2}{L^2}\sqrt{\frac{\delta L}{\pi^2} - \frac{h^2}{3}}, \tag{10}$$

at the bonding edge of the IC chip on the flexible substrate. Equation (10) indicates that the curvature at the bonding edge is only dependent of the size of the device and the compressive displacement yet independent of the material properties of the device. By introducing the thickness-length ratio $\eta = h/L$ and the compressive ratio $\lambda = \delta/L$, Eq. (10) can be further normalized as

$$\kappa_{11\max} = \frac{1}{R_{11\min}} = \frac{4\pi^2}{L}\sqrt{\frac{\lambda}{\pi^2} - \frac{\eta^2}{3}} \tag{11}$$

in which $R_{11\min}$ is the curvature radius (CR) at the bonding edge. For the sake of better intuition, CR will be used in the following discussion on the bending deformation and bendability.

It can be seen from Eq. (11) that the CR at the bonding edge is a decreasing function of the compressive ratio and an increasing function of the thickness-length ratio. As shown in Fig. 2(a), the rate of decrease in CR in the compressive ratio range of 0%–10% is much larger than that in the higher range. Moreover, for a given compressive ratio and substrate thickness, the larger the effective length, the larger the CR value. Therefore, a smaller CR value at the bonding edge can be realized in the compressive buckling experiment by increasing the compressive ratio or decreasing the effective length of the device. However, the rate of increase in CR in the thickness-length ratio range of 1%–10% is very small as shown in Fig. 2(b). Since the thickness of the flexible substrate, determined and limited by its flexibility, is usually much smaller than that of the IC chip, the influence of the thickness of the flexible substrate on the bending deformation can be neglected.

In the typical case where $L = 15$ mm, $h = 0.1$ mm, and $\delta = 8$ mm, the CR value at the bonding edge is estimated to be 1.63 mm. The working performance of the IC chip is tested following the compressive buckling, and the results are shown in Fig. 2(c), where three of four resistors lose their function. Note that the word "Unstable" marked in Fig. 2(c) refers to such a phenomenon, where the resistor functions in the flat state but fails upon very slight bending deformation. The results indicate that the CR value of 1.63 mm is beyond the bendability of the device and cannot be a safe working condition. The micro-morphology of the bonding edge is also characterized by scanning electron microscopy. Figure 2(d) shows the double cracks observed at the bonding edge: one is at the junction of the solder and the bonding pad, and the other is at the junction of the bonding pad and the polyimide substrate. The presence of double cracks can degenerate the electrical contact between the IC chip and the predefined circuit on the flexible substrate and consequently lead to failure. These two kinds of cracks can also be considered as the interfacial fracturing.

In summary, the compressive buckling method can be used to test the bendability of the IC chip-based flexible device by controlling the compressive ratio quantitatively to modulate the curvature at the bonding edge.

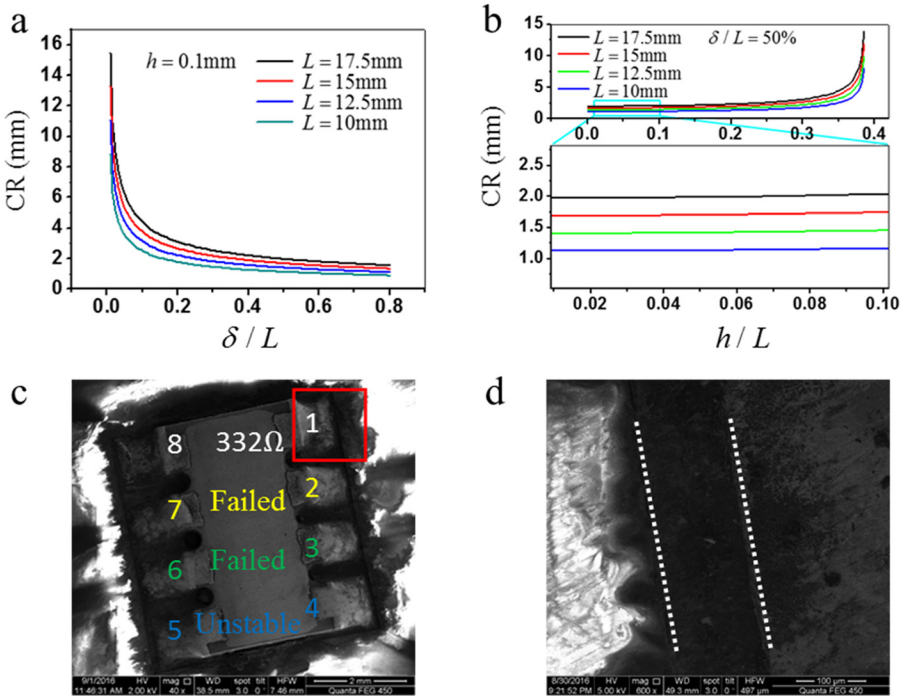

FIG. 2. The curvature radius (CR) experienced by the junction during the test and the working performance measurement after testing. (a) The dependence of the CR value on the compressive ratio, where $h = 0.1$ mm. (b) The dependence of the CR value on the thickness-length ratio. (c) The working performance testing results marked on a scanning electron micrograph of the IC chip. (d) The double cracks observed at the edge of the bonding area.

THE INTERFACIAL FAILURE MODEL

To better understand the bendability of the IC chip-based flexible devices, a theoretical model, based on the interface crack model of two elastic layers and beam theory, is developed to describe the interfacial failure between the IC chip and the flexible substrate. The main idea of the theory is to model the flexible substrate as a simple supported beam, whose critical curvature, characterizing the bendability, is determined by the interfacial strength between the IC chip and the flexible substrate. Since the bending stiffness of the IC chip is much larger than that of the flexible substrate, the substrate under the chip remains flat (i.e., the curvature and the rotation angle are both zero) when the whole device is subjected to bending. This is equivalent to the case in which the beam is subjected to two pairs of bending moments with equal magnitude satisfying the force equilibrium, as shown in Fig. 3(a).

The deformation of the flexible device in the region without IC-chip coverage is governed by

$$\bar{E} I_1 \omega'' = -M_0, \tag{12}$$

where $\bar{E}$ and I_1 are defined in the same way as those in Eqs. (3) and (6), respectively; M_0 is the bending moment per unit width, and ω is the deflection. Equation (12) shows that the critical curvature $\omega''_{\max}$ is proportional to the maximum bending moment, $M_{0\max}$, which depends on the interfacial strength.

The flexible device in the region with IC-chip coverage can be modeled as a bi-layered elastic composite with a micro-edge crack along the interface as shown in Fig. 3(b), where layer 1 denotes the flexible substrate with a thickness of h and layer 2 denotes the adhesive layer with a thickness of H. Also in Fig. 3(b), the bending moment M_1 is applied to the cross-section of layer 1 from the left side and the bending moment M_2 is applied on the cross-section of both layers from the right side. Since the bi-layered composite without an interface crack is free from any singularity under the bending loads as shown in Fig. 3(c), the superposition of such a model will not change the stress singularity of the interface crack model in Fig. 3(b). Thus, the original problem can be transformed to a new model as shown in Fig. 3(d) subjected to an equivalent bending moment $M = M_1 - C_3 M_3 = (1 - C_3) M_1$, where $M_1 = M_3$ is required by the moment equilibrium and C_3 is a dimensionless constant that depends on the material and geometric parameters. Furthermore, by using the energy method, the interfacial crack model of two elastic layers[40] shows that the energy release rate is a quadratic function of the equivalent bending moment, i.e.,

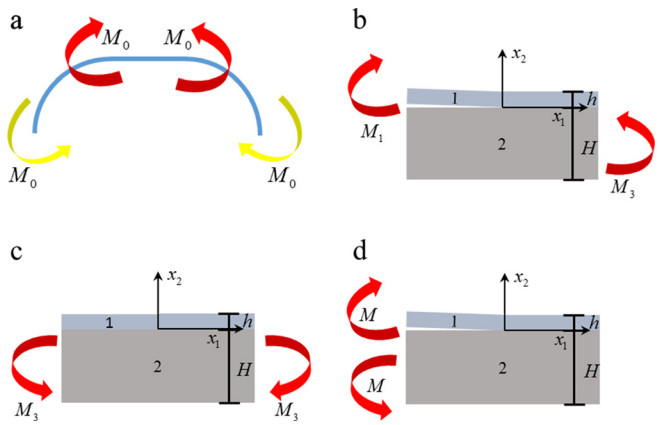

FIG. 3. Theoretical model for the IC chip integrated on the flexible substrate subjected to bending deformation. (a) The flexible substrate is modeled as the simply supported beam subjected to two pairs of bending moment with equal magnitude, M_0. (b) The interface model between the flexible substrate (layer 1) with thickness h and the adhesive layer in the IC chip (layer 2) with thickness H. (c) The crack-free bi-layered composite model subjected to a pair of bending moments, M_3. (d) The equivalent model after superposition.

$$G = \frac{c_1 M^2}{16Ih^3}, \tag{13}$$

in which c_1 and I are two known parameters that depend on the material and geometry of the two elastic layers. Due to the small thickness of the two layers, the concentrated force loaded along the interface in this loading equivalence step is neglected. In fact, the contribution of the concentrated force is estimated to be less than 7% in the energy release rate in the device discussed here.

The energy-release-rate based failure criterion indicates that once the energy release rate G exceeds the interfacial toughness G_c, the interface crack will propagate. Thus, the interfacial toughness is correlated with the critical bending deformation as

$$G_c = \frac{c_1(1-C_3)^2 \omega''^2_{\max} \bar{E}_1^2 I_1^2}{16Ih^3}. \tag{14}$$

Substituting the material and geometric parameters into Eq. (14) finally gives the analytical expression of the critical curvature as

$$\omega''_{\max} = \frac{1}{R_{\max}} = \sqrt{\frac{24G_c}{E_1 h^3}} f(\lambda', \eta', \nu_1, \nu_2), \tag{15}$$

where $R_{\max}$ is the critical curvature radius (CCR), and

$$f(\lambda', \eta', \nu_1, \nu_2) = \frac{(1-\nu_1^2)^2 + 2\lambda'\eta'(2\eta'^2 + 3\eta' + 2)(1-\nu_1^2)(1-\nu_2^2) + \lambda'^2\eta'^4(1-\nu_2^2)^2}{(1-\nu_2^2)\left[1 + \lambda'\eta'(3\eta'^2 + 6\eta' + 4)\right]\sqrt{(1-\nu_1^2) + \lambda'\eta'^3(1-\nu_2^2)}},$$

with $\eta' = h/H$ being the thickness ratio and $\lambda' = E_1/E_2$ being the modulus ratio of the two elastic layers. It is inferred from Eq. (15) that the influence of the modulus and thickness of the two layers on the critical curvature is quite different, and layer 1 (i.e., the flexible substrate) plays a dominant role as compared with layer 2 (i.e., the adhesive layer). By substituting the parameters of the aforementioned compressive buckling experiment ($E_1 = 2.5$ GPa, $E_2 = 30$ GPa, $\nu_1 = 0.34$, $\nu_2 = 0.38$, $h = 100\,\mu$m, and $H = 100\,\mu$m) into Eq. (15), we can obtain that the CCR value of the device to be 3.35 mm, which is larger than the CR value measured in the compressive buckling experiment. This fact thus explains the failure of the flexible device quantitatively.

PARAMETRIC ANALYSIS

Based on Eq. (15), the influence of the parameters in the aspects of material properties, geometric size, and interfacial toughness on the device's bendability (characterized by CCR) can be analyzed. Figures 4(a) and 4(b) show the variation of CCR with the modulus ratio for different values of E_1 and E_2, respectively. For a certain E_1, the larger E_2 leads to a smaller CCR; yet, for a certain E_2, a smaller E_1 results in a smaller CCR. Moreover, the CCR increases slowly with the increasing E_1 when $E_1/E_2 < 1$ yet relatively quickly when $E_1/E_2 \geq 1$. Therefore, decreasing E_1, increasing E_2, and keeping $E_1/E_2 < 1$ will benefit the bendability of the device. However, compared with increasing E_2, the choice of decreasing E_1 can improve the bendability of the device more efficiently due to its broader range of control and higher efficiency. In addition, when the size and interfacial toughness remain constant, the CCR value of the device that uses the soldering tin as the adhesive layer ($E_2 = 30$ GPa) in the compressive buckling experiment can be lower than 1 mm when the modulus of the flexible substrate is reduced to $E_1 = 200$ MPa.

Figures 4(c) and 4(d) show the variations of CCR with the thickness ratio, and the different colors represent different h or H. It can be observed that the CCR is negatively correlated with H for a fixed h and positively correlated with h for a fixed H. Moreover, the CCR value is more sensitive to h as compared with H. For example, the CCR variation range caused by a certain change in h is two orders of magnitude wider than that caused by the same change in H. In other words, both the decreasing thickness of the flexible substrate and the increasing thickness of the adhesive layer can improve the bendability of the device; however, the former strategy has higher efficiency. Taking the device in the compressive buckling experiment ($H = 100\,\mu$m for the adhesive layer, and the other parameters are unchanged) as an example, when the thickness of the flexible substrate is as small as 40 μm, the CCR value of the device can be reduced to 1 mm.

According to Eq. (15), we can see that the critical curvature is proportional to the square root of the interfacial toughness. The above observation follows the common sense that the tougher the interface, the smaller the CCR. Figure 5(a) shows that the CCR decreases monotonically as the interfacial toughness increases, and the rate of decrease gradually slows down to a small value quite close to zero.

Our theoretical model can not only estimate the device's CCR but also point out the most efficient way to improve the bendability of the device. Different improvement strategies, including halving the thickness of the flexible substrate, decreasing the modulus of the flexible substrate, doubling the thickness of the adhesive layer, and increasing the modulus of the adhesive layer, are compared with each other in Fig. 5(b) by taking the material and size parameters in Fig. 5(a) as the reference condition. The results indicate that the former two strategies can improve the critical curvature of the flexible substrate by around four times compared with the latter two, which show little improvement. Similarly, other possible improvements such as the increasing interfacial toughness can also be considered to find the most efficient way to enhance the bendability of the flexible device.

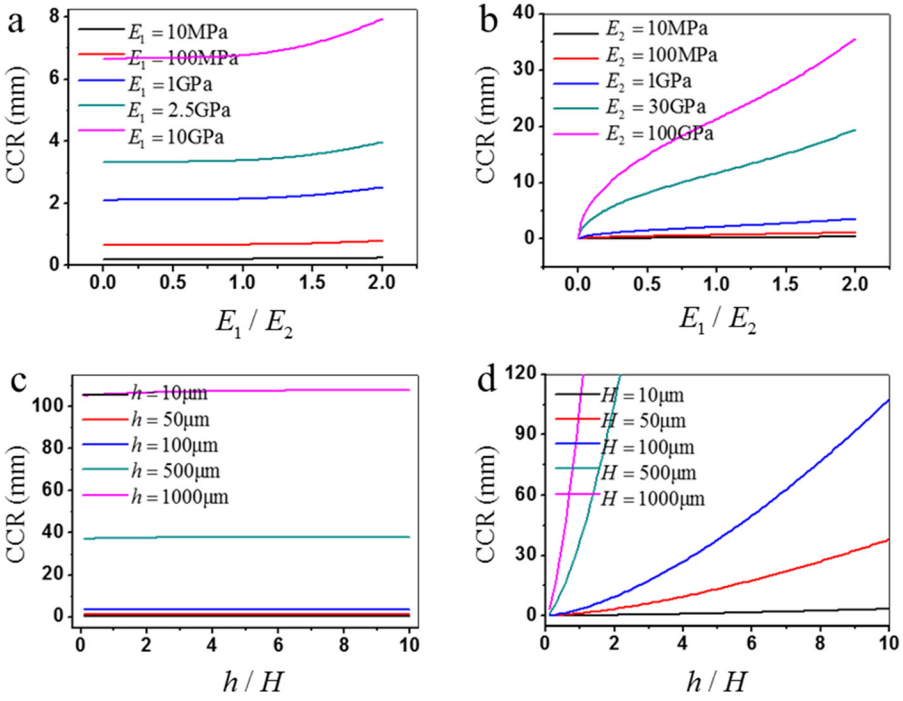

FIG. 4. The parametric analysis including modulus and thickness. (a) The relationship between the critical curvature radius (CCR) and the modulus ratio for different values of the substrate modulus, E_1. (b) The relationship between the critical curvature radius (CCR) and the modulus ratio for different values of adhesive layer modulus, E_2. (c) The relationship between the critical curvature radius (CCR) and the thickness ratio for different values of the substrate thickness, h. (d) The relationship between the critical curvature radius (CCR) and the thickness ratio for different values of the adhesive layer thickness, H.

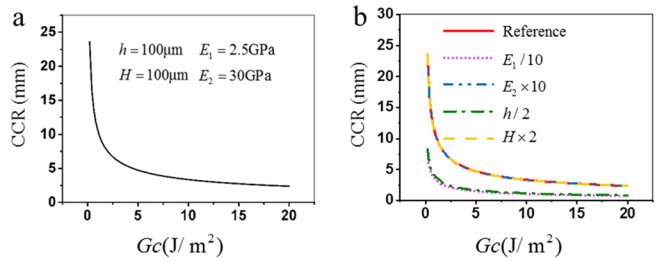

FIG. 5. Comparison between several different strategies to enhance the bendability of the device. (a) The influence of the interfacial toughness on the critical curvature radius (CCR). The parameters used here are considered as the reference ones. (b) Comparison between several improvement strategies associated with the thickness and varied values for the Young's modulus.

CONCLUSIONS

The IC chip-based flexible circuits or devices can facilitate the application of stretchable and flexible electronics for complex circuitry, such as wireless transmission, data processing, and power supply. However, the working performance and reliability of such flexible devices are shown to be highly dependent on the mechanical properties of the bonding edge of the IC chips. In this paper, we have developed an experimental method based on the compressive buckling to quantitatively impose the bending deformation onto the bonding edge of the device to test its bendability (characterized by the critical curvature). The bending load can be modulated by designing the effective length of the device or controlling the compressive ratio (i.e., the ratio of the compressive displacement to the effective length of the device). To better understand the bendability due to interfacial failure of such flexible devices, we have established a theoretical model based on the interface crack model of two elastic layers and the beam theory. This theoretical model gives the analytical expression of the critical bending curvature, above which the debonding is highly possible to occur. It turns out that decreasing the thickness and modulus of the flexible substrate, increasing the thickness and modulus of the adhesive layer, and increasing the interfacial toughness can all improve the bendability of the device. In summary, the proposed model can not only be used to estimate the bendability of a certain device but also from the detailed quantitative analysis be helpful in finding the most efficient way to enhance the device's bendability.

ACKNOWLEDGMENTS

We gratefully acknowledge the support from the National Basic Research Program of China (Grant No. 2015CB351904) and the National Natural Science Foundation of China (Grant Nos. 11625207 and 11320101001).

The authors declare no competing financial interests.

[1]Y. Zhang, Y. Huang, and J. A. Rogers, Curr. Opin. Solid State Mater. Sci. **19**, 190 (2015).
[2]J. A. Rogers, Jama **313**, 561 (2015).
[3]Y. Chen, B. W. Lu, D. P. Ou, and X. Feng, Sci. China-Phys. Mech. Astron. **58**, 594601 (2015).
[4]D. H. Kim, R. Ghaffari, N. Lu, and J. A. Rogers, Annu. Rev. Biomed. Eng. **14**, 113 (2012).
[5]D. H. Kim, J. Xiao, J. Song, Y. Huang, and J. A. Rogers, Adv. Mater. **22**, 2108 (2010).
[6]A. J. Baca, A. Jong-Hyun, S. Yugang, M. A. Meitl, M. Etienne, K. Hoon-Sik, C. Won Mook, K. Dae-Hyeong, H. Young, and J. A. Rogers, Angew. Chem. Int. Ed. **47**, 5524 (2008).
[7]T. Q. Trung, S. Ramasundaram, B. U. Hwang, and N. E. Lee, Adv. Mater. **28**, 502 (2016).
[8]J. K. Song, D. Son, J. Kim, Y. J. Yoo, G. J. Lee, L. Wang, M. K. Choi, J. Yang, M. Lee, and K. Do, Adv. Funct. Mater. **27**, 1605286 (2016).
[9]N. N. Jason, S. J. Wang, S. Bhanushali, and W. Cheng, Nanoscale **8**, 16596 (2016).
[10]Y. Chen, B. Lu, Y. Chen, and X. Feng, IEEE Electron Device Lett. **37**, 496 (2016).
[11]Y. Chen, B. Lu, Y. Chen, and X. Feng, Sci. Rep. **5**, 11505 (2015).
[12]J. Yang, D. Wei, L. Tang, X. Song, W. Luo, J. Chu, T. Gao, H. Shi, and C. Du, RSC Adv. **5**, 25609 (2015).

[13]R. C. Webb, R. M. Pielak, P. Bastien, J. Ayers, J. Niittynen, J. Kurniawan, M. Manco, A. Lin, N. H. Cho, and V. Malyrchuk, PLoS One **10**, 0118131 (2015).
[14]E. Roh, B. U. Hwang, D. Kim, B. Y. Kim, and N. E. Lee, ACS Nano **9**, 6252 (2015).
[15]C. Pang, J. H. Koo, A. Nguyen, J. M. Caves, M. G. Kim, A. Chortos, K. Kim, P. J. Wang, B. H. Tok, and Z. Bao, Adv. Mater. **27**, 634 (2015).
[16]C. M. Boutry, A. Nguyen, Q. O. Lawal, A. Chortos, S. Rondeaugagné, and Z. Bao, Adv. Mater. **27**, 6953 (2015).
[17]M. Amjadi, Y. J. Yoon, and I. Park, Nanotechnology **26**, 375501 (2015).
[18]C. M. Lochner, Y. Khan, A. Pierre, and A. C. Arias, Nat. Commun. **5**, 5745 (2014).
[19]J. Jin, H. B. R. Lee, and Z. Bao, Adv. Mater. **25**, 850 (2013).
[20]T. Yamada, Y. Hayamizu, Y. Yamamoto, Y. Yomogida, A. Izadi-Najafabadi, D. N. Futaba, and K. Hata, Nat. Nanotechnol. **6**, 296 (2011).
[21]B. Xu, A. Akhtar, Y. Liu, H. Chen, W. H. Yeo, I. S. Park, B. Boyce, H. Kim, J. Yu, and H. Y. Lai, Adv. Mater. **28**, 4462 (2016).
[22]B. Lu, Y. Chen, D. Ou, H. Chen, L. Diao, W. Zhang, J. Zheng, W. Ma, L. Sun, and X. Feng, Sci. Rep. **5**, 16065 (2015).
[23]C. Dagdeviren, B. D. Yang, Y. Su, P. L. Tran, P. Joe, E. Anderson, J. Xia, V. Doraiswamy, B. Dehdashti, and X. Feng, Proc. Natl. Acad. Sci. U.S.A. **111**, 1927 (2014).
[24]Y. Yang, H. Zhang, G. Zhu, S. Lee, Z. H. Lin, and Z. L. Wang, ACS Nano **7**, 785 (2013).
[25]D. J. Lipomi, B. C. Tee, M. Vosgueritchian, and Z. Bao, Adv. Mater. **23**, 1771 (2011).
[26]Y. Qi and M. C. Mcalpine, Energy Environ. Sci. **3**, 1275 (2010).
[27]J. Kim, P. Gutruf, A. M. Chiarelli, S. Y. Heo, K. Cho, Z. Xie, A. Banks, S. Han, K. I. Jang, and J. W. Lee, Adv. Funct. Mater. **27**, 1604373 (2016).
[28]H. Araki, J. Kim, S. Zhang, A. Banks, K. E. Crawford, X. Sheng, P. Gutruf, Y. Shi, R. M. Pielak, and J. A. Rogers, Adv. Funct. Mater. **27**, 1604465 (2017).
[29]W. Gao, S. Emaminejad, H. Y. Y. Nyein, S. Challa, K. Chen, A. Peck, H. M. Fahad, H. Ota, H. Shiraki, and D. Kiriya, Nature **529**, 509 (2016).
[30]A. Ptchelintsev, "Automated modeling and fatigue analysis of flexible printed circuits," in *Eurosime* (IEEE, 2006), p. 1.
[31]E. Martynenko, W. Zhou, A. Chudnovsky, R. S. Li, and L. Poglitsch, J. Electron. Packag. **124**, 254 (2002).
[32]W. Leong, M. Abdullah, and C. Khor, Microelectron. Reliab. **52**, 744 (2012).
[33]J. Huang, Q. Chen, L. Xu, and G. Q. Zhang, "Prediction of drop impact reliability of BGA solder joints on FPC," in *Electronics Packaging Technology Conference, Singapore* (IEEE, 2009), p. 663.
[34]L. Arruda and G. Freitas, "Effect of surrounding air on board level drop tests of flexible printed circuit boards," in EuroSime (IEEE, 2007), p. 1.
[35]E. Edqvist, N. Snis, R. C. Mohr, O. Scholz, P. Corradi, J. Gao, A. Diéguez, N. Wyrsch, and S. Johansson, J. Micromech. Microeng. **19**, 075011 (2009).
[36]Y. Wen and C. Basaran, Mech. Mater. **36**, 369 (2004).
[37]Y. Wen and C. Basaran, Int. J. Solids Struct. **40**, 3331 (2003).
[38]S. I. Park, J. H. Ahn, X. Feng, S. Wang, Y. Huang, and J. A. Rogers, Adv. Funct. Mater. **18**, 2673 (2008).
[39]L. Dai, X. Feng, B. Liu, and D. Fang, Appl. Phys. Lett. **97**, 221903 (2010).
[40]Z. Suo and J. W. Hutchinson, Int. J. Fract. **43**, 1 (1990).